Heat transfer in the transition regime: Solution of boundary value problems for Grad's moment equations via kinetic schemes

Henning Struchtrup
Department of Mechanical Engineering, University of Victoria, Victoria British Columbia, Canada V8W 3P6
(Received 31 October 2001; published 3 April 2002)

This paper presents a systematic approach to the calculation of heat transfer in rarefied gases (Knudsen numbers between 0.01 and 1) by means of Grad's moment method with high moment numbers, based on the Boltzmann equation with linearized collision term. The problem of describing boundary conditions for the moments is solved by the use of the so-called kinetic schemes that allow the implementation of the boundary condition for the Boltzmann equation. The results, obtained with up to 48 one-dimensional moment equations, exhibit temperature jumps at the walls with adjacent Knudsen boundary layers. For given wall temperatures and Knudsen number, the results change with the number of moments, and converge if the number of moments is increased.

DOI: 10.1103/PhysRevE.65.041204 PACS number(s): 51.10.+y, 44.20.+b, 44.10.+i

I. INTRODUCTION

This paper deals with models for rarefied gases in the transition regime. Here, the relevant macroscopic length scales are of the order of the magnitude of the mean free path of the gas particles, and the usual continuum models—Navier-Stokes and Fourier equations—are not applicable. Typical problems are the reentry problem of space crafts, the flow around very small objects, in particular, microelectromechanical systems (MEMS) and flow in microchannels.

Of particular interest are the forces and energy fluxes that the gas exerts on the object. Their correct calculation requires an accurate description of the effects at the boundaries, i.e., temperature jumps, velocity slip, and Knudsen boundary layers.

Processes in rarefied gases are well described by the Boltzmann equation [1,2]. The numerical solution of the Boltzmann equation, either directly [3] or via the direct simulation Monte Carlo method [4], is very time consuming [5], and there is a strong desire for accurate models that allow the calculation of processes in the transition regime at lower computational cost.

One approach towards this goal is the method of moments, due to Grad [6], in which the Boltzmann equation is replaced by a set of moment equations. In the moment method one derives a set of first-order partial-differential equations for the moments of the phase density; which and how many moments are needed depends on the particular process. Experience shows that the number of moments must be increased with increasing Knudsen number Kn (the ratio between mean free path of the molecules and relevant macroscopic length scale); sometimes one will need several hundred moments [7,8].

In this paper we shall solve moment systems for one-dimensional stationary heat transfer with up to 48 moment equations, corresponding to 430 moment equations in three-dimensional settings. The results exhibit temperature jumps at the walls and marked boundary layers. While for our problem the treatment is rather straightforward, it is evident that the number of moments is too high for applications in complex geometries and technical applications. As will become clear in the course of the paper, this high number of moments is mainly needed to avoid spurious jumps in the heat flux at the boundaries. Modified boundary conditions for the moments might be able to reduce the number of moments needed considerably, e.g., see Ref. [9]. For the present paper, however, we decided not to consider any modifications and to present the moment equations as they are. The solutions of the moment systems converge as the number of moments is increased. It should be noted that, to our best knowledge, the results presented below are the first systematic approach to solve boundary value problems for extended sets of Grad-type moment equations. For solutions of the moment equations in the bulk, i.e., under neglect of any boundary influences, see Refs. [10–12].

Only few moments have an intuitive physical meaning, i.e., density ϱ, momentum density ϱv_i, energy density ϱe, heat flux q_i, pressure tensor p_{ij}, and in an experiment only some of these can be prescribed at the boundaries. In order to clarify this point, let us consider the one-dimensional stationary heat transfer problem between rigid walls, which will be considered throughout this paper (Fig. 1). If the mass is fixed, we can successfully control four parameters: the wall temperatures T_0 and T_L, and the wall velocities $v_0 = v_L = 0$. By the physics of the problem, it is impossible to control more quantities. The heat flux q, for instance, must be adjusted so as to keep the temperatures constant and is not an independent quantity in the stationary heat transfer experiment. Alternatively, one might prescribe one of the temperatures and the heat flux q. In this case, the second temperature is not independent but will adjust itself. The mathematics of the moment equations, however, requires additional boundary values for the moments and one faces the problem to prescribe these.

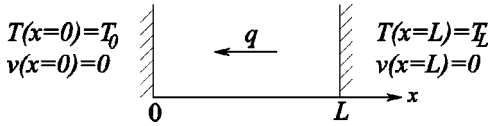

FIG. 1. Stationary heat transfer experiment between rigid walls.

Recently Le Tallec and Perlat [13] proposed a numerical scheme for the moment equations of kinetic theory. The main ingredient of this *kinetic scheme* is the use of half-space moments of the phase density; the method was introduced by Perthame to solve the Euler equations, and other hyperbolic conservation laws [14]. A similar method was discussed by Junk [15]. Within these schemes it is easy to formulate boundary conditions for the moments that follow directly from the boundary conditions for the Boltzmann equation.

While Le Tallec and Perlat use their scheme for the entropy maximum closure [16], also known as Levermore system [17], the method can be applied to any moment method of kinetic theory, e.g., in the Grad moment method [6] or in kinetic theory based extended thermodynamics [7].

In a previous paper, Ref. [9], we considered the most simple application: one-dimensional stationary heat transfer in a gas at rest, described by Grad's moment system with 13 and 14 moments [6,7]. This problem was well suited for checking the numerical scheme, since the moment equations are analytically solvable in the 13-moment case. In particular, we showed that the distance of grid points must be considerably less than the mean free path—a fact that was not recognized in [13] and [15].

However, the cases with 13 and 14 moments are appropriate for small deviations from equilibrium only and cannot be used for large Knudsen numbers. Therefore, the numerical results of [9] for large Knudsen numbers are meaningless from the physical point of view. In particular, no Knudsen boundary layers could be observed in these calculations.

In the present paper, we calculate the same process—one-dimensional stationary heat transfer—for extended sets of moments. Our moment equations are based on the Boltzmann equation with the linearized collision operator for Maxwellian molecules. The number of moments is increased until a further increase does not change the results considerably. As one might expect, it turns out that the number of moments must be larger for higher Knudsen numbers and higher temperature gradients.

As in [9], our results exhibit temperature jumps at the walls. A particular feature of the given results is the occurrence of boundary layers (Knudsen layers) [18,3], accompanied by anisotropic stresses. These anisotropic stresses are not driven by velocity gradients—the velocity is zero—so that this effect cannot be described within the Navier-Stokes-Fourier theory. A similar effect is a heat flux without temperature gradient in the case of parallel Couette flow, see [19,20]. In our previous calculations [9], the kinetic schemes did not preserve the energy at the walls. We gave arguments that this behavior should change when a larger number of moments is taken into account and this is indeed the case. Still, one observes jumps in the heat flux at the walls, but while the jump is about 5% in the 13-moments case of [9], it goes down to 0.3% for the 148-moment case (24 equations in the one-dimensional problem).

Temperature jumps and slip are easily incorporated into the Navier-Stokes-Fourier theory [2] that, however, does not describe Knudsen layers. The Navier-Stokes-Fourier theory follows from the Chapman-Enskog expansion of the Boltzmann equation into first order of the Knudsen number [1,2]. One might expect that Chapman-Enskog expansions to higher orders, i.e., the Burnett and Super-Burnett equations [2,21], are appropriate for the description of boundary value problems in rarefied gases. This, however, is not true: Apart from the known problems of the Burnett equations, such as instability [22,23] and violations of the second law [24,25], they do not describe linear boundary layers [26] and must be supplemented by an appropriate boundary layer theory [1,27]. See also Ref. [28] for the asymptotic theory of boundary value problems for the Boltzmann equation.

In [5] the authors compute boundary layers from the Burnett equations. A closer examination shows that these are due to nonlinear terms in the equations and can only be seen in the case of the strong gradients applied in that paper. The Knudsen boundary layers, which we shall compute from the moment equations, are due to linear terms and will be observed also if the gradients are weak.

Our approach focuses on the interplay between the bulk behavior of the gas and the influences of the boundaries. In other papers, the authors try to extract the bulk behavior alone [10–12,29,30]; these results cannot be compared with our results.

The problem of boundary values for higher moments can also be tackled with a minimax principle for the entropy production, due to Struchtrup and Weiss [31], see [20,32–34] for applications. This method gives qualitatively good results, but its status remains unclear, since so far it was not shown that the results are also *quantitatively* correct. The results presented here may be used for comparison. It must be noted, however, that already in case of a low moment number the application of this principle is forbiddingly complicated, and that it will be almost impossible to use it in the case of the large moment numbers considered here.

The paper is organized as follows. The following section gives a brief introduction to moment systems of kinetic theory. Section III deals with the heat transfer experiment. We simplify the equations, introduce appropriate dimensionless variables, and discuss the moment equations for 13 and 26 moments. In Sec. IV we present our derivation of the kinetic scheme. The application of the scheme to the heat transfer problem with an arbitrary number of moments and a detailed discussion of the results will be found in Sec. V. The paper ends with our conclusions.

II. MOMENT SYSTEMS OF KINETIC THEORY

A. Kinetic theory

We consider one-atomic ideal gases. The objective of the kinetic theory of gases is the determination of the phase density $f(x_i,t,c_i)$ that gives the number of particles in the phase space element $d\boldsymbol{x}\,d\boldsymbol{c}$. Here, x_i,t denote space and time variables, respectively, and c_i is the velocity of a particle of mass m. The phase density is governed by the Boltzmann equation [1,2]

$$\frac{\partial f}{\partial t}+c_k\frac{\partial f}{\partial x_k}=\mathcal{S}(f), \tag{1}$$

where the collision term $\mathcal{S}(f)$ accounts for the change of the phase density due to collisions among particles.

Once the phase density is known, one may calculate its moments, for instance, the mass density ϱ, the momentum density ϱv_i, and the energy density $\varrho\varepsilon$, given by

$$\varrho = m\int f\, d\boldsymbol{c}, \quad \varrho v_i = m\int c_i f\, d\boldsymbol{c},$$

$$\varrho\varepsilon = \frac{3}{2}\varrho\frac{k}{m}T + \frac{\varrho}{2}v^2 = \frac{m}{2}\int c^2 f\, d\boldsymbol{c}. \tag{2}$$

In these definitions, k is Boltzmann's constant, v_i denotes the barycentric velocity of the gas and T denotes the temperature, which is *defined* here.

Pressure tensor p_{ij} and heat flux vector q_i are given by

$$p_{ij} = p\,\delta_{ij} + p_{\langle ij\rangle} = m\int C_i C_j f\, d\boldsymbol{c}, \quad q_i = \frac{m}{2}\int C^2 C_i f\, d\boldsymbol{c},$$

where $C_i = c_i - v_i$ is the peculiar velocity. By comparison with Eqs. (2) the pressure is related to temperature and density by the ideal gas law, $p = \varrho(k/m)T$. The pressure deviator is denoted by $p_{\langle ij\rangle}$; the brackets label the traceless part of a symmetric tensor.

B. Maxwell's boundary conditions

For the calculation of boundary value problems, one needs boundary conditions for the phase density f. The most simple model for these goes back to Maxwell [1,2]. He assumes that the fraction $(1-\theta)$ of the emerging particles is reflected elastically at the wall. The remaining fraction θ is thermalized and leaves the wall in a Maxwellian distribution. θ is called accommodation coefficient.

We denote the velocity of a particle by c_i and the velocity of the wall by v_i^W, such that the particle has the velocity $C_i^W = c_i - v_i^W$ in the frame where the wall is at rest. Moreover, we choose the normal vector n_i of the wall so that it points inside the gas such that we have $n_k C_k^W \leqslant 0$ for the emerging particles and $n_k C_k^W \geqslant 0$ for the particles that leave the wall.

Furthermore, $f_N(C_i^W, x_i, t)$ denotes the phase density inside the gas in front of the wall. For our purposes it is convenient to write f_N as a function of the tangential velocity $C_i^W - n_k C_k^W n_i$ and the normal velocity $n_k C_k^W$ as $f_N(C_i^W - n_k C_k^W n_i, n_k C_k^W, x_i, t)$. In an elastic collision, the tangential velocity remains unchanged, while the normal velocity changes its sign. So we have the phase densities $f_N(C_i^W - n_k C_k^W n_i, n_k C_k^W, x_i, t)$ for the emerging particles $(n_k C_k^W \leqslant 0)$ and $f_N(C_i^W - n_k C_k^W n_i, -n_k C_k^W, x_i, t)$ for the elastically reflected particles $(n_k C_k^W \geqslant 0)$, respectively. In the following, for simplicity of the notation, we suppress the tangential velocity as well as space and time in the list of arguments of f_N and write the phase density directly at the wall $\hat{f}$ according to Maxwells boundary conditions as

$$\hat{f} = \begin{cases} \theta f_W + (1-\theta) f_N(-n_k C_k^W), & n_k C_k^W \geqslant 0, \\ f_N(n_k C_k^W), & n_k C_k^W \leqslant 0, \end{cases} \tag{3}$$

f_W is the Maxwellian of the thermalized particles,

$$f_W = f_M(\varrho_W, T_W, v_i^W) = \frac{\varrho_W}{m}\left(\sqrt{\frac{m}{2\pi k T_W}}\right)^3 \times \exp\left[-\frac{m}{2kT_W}(c_k - v_k^W)^2\right],$$

where T_W denotes the temperature of the wall and ϱ_W is the density of the thermalized particles. ϱ_W has be to determined in order to ensure that the wall does not accumulate particles, a condition that may be written as

$$m\int_{n_k C_k^W \geqslant 0} \hat{f} C_k^W n_k\, d\boldsymbol{c} = -m\int_{n_k C_k^W \leqslant 0} \hat{f} C_k^W n_k\, d\boldsymbol{c}. \tag{4}$$

In the remainder of this paper we consider a gas at rest only, so that $\int f_N c_k n_k\, d\boldsymbol{c} = 0$. Of course, in this case also the walls are at rest, $v_k^W = 0$ and the condition (4) simplifies to

$$m\int_{c_k n_k \geqslant 0} f_W c_k n_k\, d\boldsymbol{c} = m\int_{c_k n_k \geqslant 0} f_N c_k n_k\, d\boldsymbol{c}. \tag{5}$$

C. Moments and moment equations

In moment methods one assumes that the state of the gas is satisfactorily described by a set of moments

$$u_A = \int \Psi_A(c_k) f\, d\boldsymbol{c},$$

where $\Psi_A(c_k)$ is a vector of polynomials of the microscopic velocity. Which moments one has to take into account depends on the process under consideration. In Grad's 13-moment theory, one has $\Psi_A = m\{1, c_i, \frac{1}{2}c^2, c_{\langle i}c_{j\rangle}, \frac{1}{2}c^2 c_i\}$, i.e., the moments $\varrho, \varrho v_i, \varrho\varepsilon, p_{\langle ij\rangle}, q_i$ defined above.

Multiplication of the Boltzmann Eq. (1) by Ψ_A and subsequent integration over velocity space yields the moment equations

$$\frac{\partial u_A}{\partial t} + \frac{\partial F_{Ak}}{\partial x_k} = P_A \quad \text{with} \quad F_{Ak} = \int \Psi_A c_k f\, d\boldsymbol{c}, \tag{6a}$$

$$P_A = \int \Psi_A \mathcal{S} f\, d\boldsymbol{c}, \tag{6b}$$

where we have introduced the fluxes of the moments F_{Ak} and their productions P_A. Note that the productions of mass, momentum, and energy vanish.

The Eqs. (6a) do not form a closed system of partial differential equations for the moments since they contain the fluxes and the productions which are not *a priori* related to the moments. Here, a closure assumption is required, and it is obvious that a phase density of the form

$$f(x_k, t, c_k) = f(u_A(x_k, t), c_k) \tag{7}$$

serves for this purpose. In the sequel, a solution of this type will be called ''moment solution.'' There are several methods to obtain a solution of this type. Grad found his moment solution by an expansion around local equilibrium where the phase density is a Maxwellian. In recent years, the methods of maximizing the entropy [16,17,27] and the equivalent method of extended thermodynamics [7] became more and more popular. These methods may lead to ill-posed problems [15,35] and in Ref. [35] it is shown that the Grad method gives results in accordance with the Boltzmann equation, while the entropy maximum method does not. One of the shortcomings of the moment theory is that it is not clear which boundary conditions one has to choose for moments without physical meaning, a problem that was addressed in Ref. [31]. The numerical scheme of Le Tallec and Perlat, discussed in Sec. IV below, allows the use of boundary condition (3) for the phase density in its implementation. Thus, it will be possible to solve problems of kinetic theory with an arbitrary number of moments.

D. Choice of moments

The set of 13 moments contains the only moments that have an intuitive physical meaning. With no physical meaning for the other moments, it raises the question, which moments one should consider for extended moment systems. *A priori*, there are no restrictions on the choice of moments, but in order to have a somewhat systematic approach we choose the sets of moments by the following argument.

The basic quantities are the conserved quantities, mass, momentum, and energy, given by

$$u_A^{[5]}=\int \Psi_A^{[5]} f\, d\boldsymbol{c} \quad \text{with} \quad \Psi_A^{[5]}=m\{1,c_i,c^2\}.$$

In order to close the system, we have either to find constitutive equations for pressure tensor and heat flux [43], or we can add these to the list of variables, i.e., choose

$$u_A^{[13]}=\int \Psi_A^{[13]} f\, d\boldsymbol{c} \quad \text{with} \quad \Psi_A^{[13]}=m\{1,c_i,c_ic_j,c^2c_j\}.$$

A closer look shows that in this case we need additional equations for the fluxes of heat flux and pressure tensor, i.e., for $\int c_{\langle i}c_{j\rangle}c_k f\, d\boldsymbol{c}$ and $\int c^2c_ic_k f\, d\boldsymbol{c}$. Again, we have either to find constitutive equations for these fluxes, or we can add them to the list of variables. If we proceed in this manner, we come to the following choices of moments:

$$\Psi_A^{(\alpha)}=m\{1,c_i,c_ic_j,\ldots,c_{i_1}c_{i_2}\cdots c_{i_\alpha},c^2c_{i_1}c_{i_2}\cdots c_{i_{\alpha-1}}\},$$

$$\alpha=2,3,\ldots,11 \tag{8}$$

corresponding to 13 (5), 26 (8), 45 (11), 71 (15), 105 (19), 148 (24), 201 (29), 265 (35), 341 (41), and 430 (48) moments; the numbers in parentheses indicate the number of partial-differential equations, which must be solved in the one-dimensional case. In the sequel, we shall identify the sets of moment equations by the number of equations for the one-dimensional case, i.e., the Euler equations are the three-moment case, Grad's 13-moment equations will be referred to as the five-moment case and so on. In this paper we shall not go beyond the 48-moment case ($\alpha=11$).

In the moment theory, one usually makes the barycentric velocity explicit, and builds up the moments with the peculiar velocity $C_i=c_i-v_i$, instead of the particle velocity c_i. We shall consider gases at rest exclusively, where $v_i=0$ at all times. Then, obviously, both velocities, C_i and c_i, agree.

E. Grad distribution

In Grad's moment method, the phase density is related to the moments as

$$f^{(\alpha)}=f_M\left(1+\sum_A \Lambda_A^{(\alpha)}(u_B)\Psi_A^{(\alpha)}\right)$$

with

$$u_A=\int \Psi_A^{(\alpha)} f^{(\alpha)} d\boldsymbol{c}; \tag{9}$$

the coefficients $\Lambda_A^{(\alpha)}$ follow from the inversion of the last equation. f_M denotes the local Maxwellian, given by

$$f_M=\frac{\varrho}{m}\left(\sqrt{\frac{m}{2\pi kT}}\right)^3 \exp\left[-\frac{m}{2kT}(c_k-v_k)^2\right].$$

Equation (9) is the requested moment solution, and will be used to compute the constitutive functions for fluxes and productions as

$$F_{Ak}(x_i,t)=F_{Ak}(u_B(x_i,t)), \quad P_A(x_i,t)=P_A(u_B(x_i,t)).$$

The constitutive functions are local, i.e., depend only on the local values of the moments u_A, and not on gradients or time derivatives of the moments.

F. One-dimensional processes

We shall consider only one-dimensional processes where all fields depend on the space variable $x_1=x$, and all fluxes point in the same direction. We have to identify the relevant variables for this case. To this objective, we decompose the moments $u_{i_1i_2\ldots i_n}$ into their irreducible parts, i.e., into their traces and trace-free parts [8,36]. We define

$$u^{(k)}_{\langle i_1i_2\cdots i_n\rangle}=m\int c^{2k}c_{\langle i_1\cdots i_n\rangle} f\, d\boldsymbol{c} \quad \text{with}$$

$$u^k_{\langle i_1i_2\cdots i_n\rangle}\delta_{i_ji_k}=0$$

and have

$$u_{i_1i_2,\ldots,i_n}=\sum_{k=0}^{\|n/2\|}\hat{b}_{n,k}[\,\delta_{i_1i_2}\cdots\delta_{i_{2k-1}i_{2k}}u^{(k)}_{\langle i_{2k+1}\cdots i_n\rangle}$$

$$+\cdots(P_{nk}\text{terms})],$$

where $u^{(k)}_{\langle i_{2k+1}\cdots i_n\rangle}$ is the trace-free part of the kth trace of $u_{i_1\cdots i_n}$. The sum in the brackets extends over all different permutations of the indices and

$$\hat{b}_{n,k}=\frac{1}{\prod_{j=0}^{k-1}(2(n-k-j)+1)},$$

$$P_{n,k}=\frac{n!}{(n-2k)!2^k k!},\quad \left\|\frac{n}{2}\right\|=\begin{cases}\dfrac{n}{2}, & n \text{ even}\\ \dfrac{n-1}{2}, & n \text{ uneven.}\end{cases}$$

The first few tensors $u_{i_1\cdots i_n}$ decompose according to

$$u_i=u^{(0)}_{\langle i\rangle}$$

$$u_{ij}=u^{(0)}_{\langle ij\rangle}+\tfrac{1}{3}u^{(1)}\delta_{ij}$$

$$u_{ijk}=u^{(0)}_{\langle ijk\rangle}+\tfrac{1}{5}(u^{(1)}_i\delta_{jk}+u^{(1)}_j\delta_{ik}+u^{(1)}_k\delta_{ij}).$$

In the one-dimensional case, one needs to consider only the $x,\ldots,x$ parts of the trace-free moments. Thus, we define

$$\psi^{(k)}_{\langle n\rangle}=m\sum_{r=0}^{\|n/2\|}\frac{(-1)^r}{\prod_{j=0}^{r-1}(2n-2j-1)}\frac{n!}{(n-2r)!2^r r!}c^{2(r+k)}c_x^{n-2r} \tag{10}$$

and have the variables, fluxes, and productions for the one-dimensional case given by

$$u^{(k)}_{\langle n\rangle}=\underbrace{u^{(k)}_{\langle xx\cdots x\rangle}}_{n \text{ times}}=\int \psi^{(k)}_{\langle n\rangle} f\, d\mathbf{c}, \tag{11a}$$

$$F^{(k)}_{\langle n\rangle}=\int \psi^{(k)}_{\langle n\rangle} c_x f\, d\mathbf{c}, \tag{11b}$$

$$P^{(k)}_{\langle n\rangle}=\int \psi^{(k)}_{\langle n\rangle}\mathcal{S}\, d\mathbf{c}. \tag{11c}$$

The choice (8) of moments corresponds to the set of variables

$$u^{(k)}_{\langle n-2k\rangle},\quad k=0,\ldots,\left\|\frac{n}{2}\right\|,\quad n=0,\ldots,\alpha$$

$$u^{(k)}_{\langle \alpha+1-2k\rangle},\quad k=1,\ldots,\left\|\frac{\alpha+1}{2}\right\|.$$

The one-dimensional moment equations read

$$\frac{\partial u^{(k)}_{\langle n\rangle}}{\partial t}+\frac{\partial F^{(k)}_{\langle n\rangle}}{\partial x}=P^{(k)}_{\langle n\rangle} \tag{12}$$

and the phase density is now given by

$$f=f_M\left(1+\sum_{k,n}\lambda^{(k)}_{\langle n\rangle}\psi^{(k)}_{\langle n\rangle}\right). \tag{13}$$

The parameters $\lambda^{(k)}_{\langle n\rangle}$ are functions of the moments $u^{(k)}_{\langle n\rangle}$ and follow from insertion of Eq. (13) in Eq. (11a) and inversion. The trace-free tensors $\psi^{(k)}_{\langle n\rangle}$ are related to spherical harmonics [36], and are orthogonal with respect to integration over the Maxwellian, $\int f_M\psi^{(k)}_{\langle n\rangle}\psi^{(l)}_{\langle m\rangle}d\mathbf{c}=a_{kl}\delta_{nm}$. This property simplifies the calculation of the coefficients $\lambda^{(k)}_{\langle n\rangle}$ considerably. We shall not give any detail of these calculations, which were performed by means of the computer algebra system MATHEMATICA®.

The productions $P^{(k)}_{\langle n\rangle}$ depend on the choice of the collision term $\mathcal{S}(f)$. Here, we have adopted the linearized collision term for Maxwell molecules, which is evaluated in Ref. [36] via its eigenfunctions (Sonine polynomials). Our functions $\psi^{(k)}_{\langle n\rangle}$ are linear combinations of the eigenfunctions, and thus, the corresponding productions are linear combinations of the production terms for the eigenfunctions. These calculations were performed with another MATHEMATICA® program, developed by Au in the context of his thesis [37].

The computation of the production terms for other laws of interaction between atoms, e.g., hard sphere molecules, or Lenneard-Jones particles, is possible in principle. We chose Maxwell molecules here, since the use of the eigenfunction method allows a very fast and elegant approach to the computation of production terms, while other interaction potentials require the term-by-term integration of the productions. Ohwada [18] notices that the heat transfer problem is not influenced much by the change of the interaction potential. This will be confirmed by the comparison of our results with Ohwada's in Sec. V C below.

The computation of the productions is even more involved for the full nonlinear Boltzmann collision term. While, for Maxwell molecules, it is possible to compute the productions without knowledge of the phase density, our attempts to find a general equation for the nonlinear production for arbitrary moments failed so far. See Ref. [38] for the computation of nonlinear production terms for some higher moments.

We shall not give details of the computation of the productions. However, in order to gain an idea of the form and dimensions of the productions, it is useful to have a look on the productions according to the BGK model [1,39]. If we adopt the mean collision frequency for Maxwell molecules, the BGK collision term reads

$$\mathcal{S}(f)=-\varrho\,\gamma(f-f_M).$$

Here, γ is a constant that follows from the calculation of the collision production for Maxwell molecules, and $\varrho\,\gamma$ is the collision frequency. Obviously, the productions for the BGK model read

$$P^{(k)}_{\langle n\rangle}=-\varrho\,\gamma(u^{(k)}_{\langle n\rangle}-u^{(k)}_{\langle n\rangle|E}); \tag{14}$$

$u^{(k)}_{\langle n\rangle|E}$ denotes the moments of the local Maxwellian. γ is related to the heat conductivity κ by

$$\kappa=\frac{15}{4}\left(\frac{k}{m}\right)^2\frac{T}{\gamma}, \tag{15}$$

where γ is chosen in order to give the proper heat conductivity for Maxwell molecules. Note that the BGK-model

gives the wrong Prandtl number $\mathrm{Pr}=(5/2)(k/m)(\mu/\kappa)$ where μ is the viscosity. The Prandtl number for Maxwellian molecules is $\mathrm{Pr}=2/3$ while the BGK model gives $\mathrm{Pr}=1$. Thus, with Eq. (15), the viscosity has an improper value. The BGK production terms are not used for our numerical simulations below, which rely on the true productions of Maxwell molecules.

III. STATIONARY HEAT TRANSFER

A. Basic equations

We consider the stationary heat transfer experiment, as depicted in Fig. 1. As in Ref. [9], we shall compute the stationary state via time stepping of the kinetic scheme. Therefore, we are interested in the time-dependent moment equations. Following the same lines as in Ref. [9], we shall reduce the equations due to our knowledge of the stationary result.

First, we consider the balance equations for the conserved quantities, mass, momentum, and energy. In the one-dimensional case, they read

$$\frac{\partial \varrho}{\partial t}+\frac{\partial \varrho v}{\partial x}=0,$$

$$\frac{\partial \varrho v}{\partial t}+\frac{\partial(\varrho v^2+p+\sigma)}{\partial x}=0,$$

$$\frac{\partial\left(\frac{3}{2}\varrho\frac{k}{m}T+\frac{\varrho}{2}v^2\right)}{\partial t}+\frac{\partial\left[\left(\frac{3}{2}\varrho\frac{k}{m}T+\frac{\varrho}{2}v^2\right)v+q+(p+\sigma)v\right]}{\partial x}=0.$$

Here, $\varrho=u^{(0)}_{\langle 0\rangle}$ is the density, $T=\frac{1}{3}u^{(1)}_{\langle 0\rangle}/u^{(0)}_{\langle 0\rangle}(k/m)$ is the temperature, $v=u^{(0)}_{\langle 1\rangle}$ is the velocity, $\sigma=u^{(0)}_{\langle 2\rangle}$ is the $\langle xx\rangle$ component of the pressure tensor, and $q=\frac{1}{2}u^{(1)}_{\langle 1\rangle}$ is the $\langle x\rangle$ component of the heat flux. By means of mass and momentum balance, the energy balance can be reduced to the balance of internal energy, viz.,

$$\varrho\frac{\partial\frac{3}{2}\frac{k}{m}T}{\partial t}+\varrho v\frac{\partial\frac{3}{2}\frac{k}{m}T}{\partial x}+\frac{\partial q}{\partial x}+(p+\sigma)\frac{\partial v}{\partial x}=0.$$

Since the walls do not move, the gas will be at rest in the stationary state, so that the velocity vanishes, $v=0$. Then, the momentum balance reduces to $\partial(p+\sigma)/\partial x=0$ and integration gives

$$p+\sigma=p_0, \tag{16}$$

where p_0 is a constant of the dimension of pressure. Other authors solve the heat transfer problem in the bulk [10–12], i.e., without considering any boundary conditions, under the assumption that the pressure p is constant so that $\sigma=0$. In our treatment, σ is a variable in its own right and its values will follow from the solution of the boundary value problem. Note, however, that there is no physical argument to assume $\sigma=0$ even far away from any boundaries.

Henceforth, we shall not consider the nonstationary conservation laws for mass and momentum but replace them by their stationary form, i.e.,

$$v=u^{(0)}_{\langle 1\rangle}=0 \quad \text{and} \quad \varrho=u^{(0)}_{\langle 0\rangle}=\frac{p_0-\sigma}{\frac{k}{m}T}; \tag{17}$$

the last equation follows from Eq. (16) by means of the ideal gas law. Accordingly, the balance of internal energy reads

$$\frac{3}{2}(p_0-\sigma)\frac{\partial \ln T}{\partial t}+\frac{\partial q}{\partial x}=0. \tag{18}$$

Next, we introduce dimensionless variables. The length scale is defined by the wall distance L, and we choose a temperature T_0 as the measure for temperature. In most of our calculations, T_0 will be the temperature of the left wall. The constant of integration p_0 defines the scale for the density as $\varrho_0=p_0/(k/m)T_0$. The velocity scale is given by $\sqrt{(k/m)T_0}$ and defines also the time scale by $L/\sqrt{(k/m)T_0}$. Altogether, we introduce the following dimensionless quantities:

$$\hat{x}=\frac{x}{L}, \quad \hat{t}=\frac{\sqrt{\frac{k}{m}T_0}t}{L}, \quad \hat{c}_i=\frac{c_i}{\sqrt{\frac{k}{m}T_0}}, \quad \hat{T}=\frac{T}{T_0},$$

$$\hat{u}^{(k)}_{\langle n\rangle}=\frac{u^{(k)}_{\langle n\rangle}}{p_0\left(\sqrt{\frac{k}{m}T_0}\right)^{2k+n-2}}.$$

The dimensionless productions contain the Knudsen number given by

$$\mathrm{Kn}=\frac{\sqrt{\frac{k}{m}T_0}^3}{Lp_0\gamma}. \tag{19}$$

We find the following dimensionless formulation: Velocity and density are eliminated by

$$\hat{v}=u^{(0)}_{\langle 1\rangle}=0, \quad \hat{\varrho}=\frac{1-\hat{\sigma}}{\hat{T}};$$

the evolution of temperature follows from

$$\frac{3}{2}(1-\hat{\sigma})\frac{\partial \ln \hat{T}}{\partial \hat{t}}+\frac{\partial \hat{q}}{\partial \hat{x}}=0, \tag{20}$$

all other moments obey the evolution equation

$$\frac{\partial \hat{u}_{\langle n\rangle}^{(k)}}{\partial \hat{t}}+\frac{\partial \hat{F}_{\langle n\rangle}^{(k)}}{\partial \hat{x}}=\hat{P}_{\langle n\rangle}^{(k)},$$

and the phase density for the closure is given by

$$\hat{f}=\frac{1-\hat{\sigma}}{\hat{T}}\left(\sqrt{\frac{1}{2\pi\hat{T}}}\right)^{3} e^{-\hat{c}^2/2\hat{T}}\left(1+\sum_{k,n}\hat{\lambda}_{\langle n\rangle}^{(k)}\hat{\psi}_{\langle n\rangle}^{(k)}\right). \quad (21)$$

$\hat{\psi}_{\langle n\rangle}^{(k)}$ is the same function as $\psi_{\langle n\rangle}^{(k)}$ but with $m=1$ and the dimensionless velocity $\hat{c}_i$. The closure procedure is as before: the dimensionless coefficients $\hat{\lambda}_{\langle n\rangle}^{(k)}$ are computed by insertion of Eq. (21) into Eq. (11a) and then Eqs. (11b),(11c) give the dimensionless constitutive equations.

For the BGK case the productions read

$$\hat{P}_{\langle n\rangle}^{(k)}=-\frac{1}{\mathrm{Kn}}\frac{1-\hat{\sigma}}{\hat{T}}(\hat{u}_{\langle n\rangle}^{(k)}-\hat{u}_{\langle n\rangle|E}^{(k)}).$$

We emphasize again that our numerical calculations rely on the true productions of Maxwell molecules, the BGK terms are only introduced to give a flavor of their dependence on the variables.

The hats that characterize the dimensionless quantities will be omitted in the sequel.

B. Stationary heat transfer with five moments

Before we consider the numerical solution of the moment equations via kinetic schemes, we study the heat transfer with five and eight moments in some detail. For the purpose of the following two sections, we consider complete accommodation, i.e., $\theta=0$. We start with the stationary state of the five-moment case (Grad's 13-moment case), where the moment equations for energy, pressure tensor, and heat flux read

$$\frac{\partial q}{\partial x}=0,$$

$$\frac{8}{15}\frac{\partial q}{\partial x}=-\frac{1}{\mathrm{Kn}}\frac{(1-\sigma)\sigma}{T},$$

$$\frac{\partial}{\partial x}(5T+2T\sigma)=-\frac{4}{3\mathrm{Kn}}\frac{(1-\sigma)q}{T}.$$

The first two equations show that the anisotropic stress vanishes, $\sigma=0$, and the equations reduce simply to the law of Fourier

$$q=-\frac{15}{4}\mathrm{Kn}\,T\frac{\partial T}{\partial x}=\mathrm{const}. \quad (22)$$

Notice that the (dimensionless) heat conductivity $\frac{15}{4}\mathrm{Kn}\,T$ depends on the temperature. We prescribe $T(x=0)=\vartheta_0$ and $T(x=1)=\vartheta_L$ to obtain

$$T=\sqrt{\vartheta_0^2+(\vartheta_L^2-\vartheta_0^2)x}, \quad (23a)$$

$$q=-\frac{15}{8}\mathrm{Kn}(\vartheta_L^2-\vartheta_0^2). \quad (23b)$$

The temperatures ϑ_0,ϑ_L are not the temperatures of the walls, but the temperatures of the gas directly at the walls and differ from the wall temperatures $T_0=1,T_L$. Indeed, in the case of large Knudsen numbers one has to consider the jump of the temperature at a wall and we proceed with its calculation [2,9,32]. To this end, we consider the boundary condition (3) for gas and boundary at rest, written in dimensionless form. The normal part of the energy flux $\frac{1}{2}\int c^2 c_i f\,d\boldsymbol{c}$ has to be continuous at the wall, a condition that we may write as $\frac{1}{2}\int \hat{f}c^2c_k n_k\,d\boldsymbol{c}=\frac{1}{2}\int f_N c^2 c_k n_k\,d\boldsymbol{c}$ or, with Eq. (3),

$$\frac{1}{2}\int_{n_k c_k\geqslant 0} f_W c^2 c_k n_k\,d\boldsymbol{c}=\frac{1}{2}\int_{n_k c_k\geqslant 0} f_N c^2 c_k\,d\boldsymbol{c}. \quad (24)$$

Now we consider Grad's 13-moments phase density with vanishing shear stresses, as it is appropriate in stationary heat transfer, viz.,

$$f^{[5]}=\frac{1}{\vartheta}\sqrt{\frac{1}{2\pi\vartheta}}^{3} e^{-c^2/2\vartheta}\left[1-\frac{q_x c_x}{\vartheta}\left(1-\frac{1}{5}\frac{c^2}{\vartheta}\right)\right],$$

where ϑ is the temperature of the gas at the wall. We obtain from the conditions for conservation of mass and heat flux (5) and (24)

$$\sqrt{\frac{1}{2\pi}}\varrho_W\sqrt{T_W}=\sqrt{\frac{1}{2\pi}}\sqrt{\frac{1}{\vartheta}},$$

$$\varrho_W\sqrt{\frac{2}{\pi}}\sqrt{T_W}^3=\sqrt{\frac{2}{\pi}}\sqrt{\vartheta}+\frac{1}{2}q_x n_x.$$

Elimination of the density ϱ_W yields for the temperature jumps at $x=0$, $x=1$,

$$\frac{1-\vartheta_0}{\vartheta_0}=\frac{1}{2}\sqrt{\frac{\pi}{2}}\frac{q}{\sqrt{\vartheta_0}},\quad \frac{T_L-\vartheta_L}{\vartheta_L}=-\frac{1}{2}\sqrt{\frac{\pi}{2}}\frac{q}{\sqrt{\vartheta_L}}. \quad (25)$$

ϑ_0 and ϑ_L follow from Eq. (25) with Eq. (23b). In the remainder of the paper we shall calculate the stationary heat transfer problem with numerical methods and we shall use Eqs. (23a) and (23b) for comparison. Figure 2 shows the temperature for various Knudsen numbers (wall temperatures $T_0=1,T_L=1.5$). The jumps increase with increasing Knudsen number.

C. Stationary heat transfer with eight moments

Although there are jumps, no Knudsen boundary layers are present in the five-moment case. Indeed, while the temperature jumps depend on the Knudsen number [see Eq. (25)], the temperature profile as given by Eqs. (23a) is independent of the Knudsen number, that is, it depends only on the temperatures ϑ_0,ϑ_L at the wall, but has no explicit de-

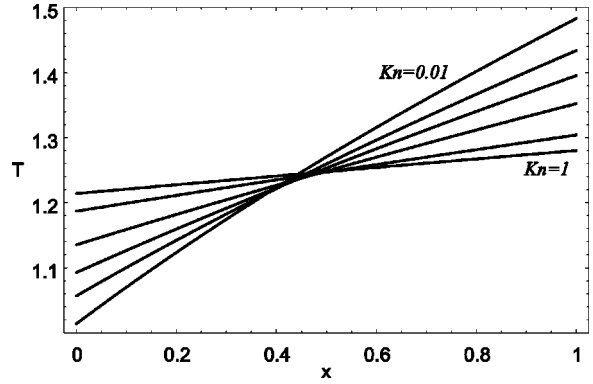

FIG. 2. Temperature according to Fourier's law with temperature jumps for Knudsen numbers Kn=0.01,0.05,0.1,0.2,0.5,1; wall temperatures $T_0=1$, $T_L=1.5$.

pendence on the Knudsen number. The curvature is solely due to the temperature dependence of the heat conductivity.

When more moments are taken into account, the temperature profile will again depend on the temperatures at the walls (the temperature jumps) but will also contain contributions that are *explicit* in the Knudsen number. This will be seen when we study the next member of our moment sets, i.e., the eight moment case [corresponding to 26 moments in three dimensions (3D)]. The equations follow from the procedures described above as (stationary case)

$$\frac{\partial q}{\partial x}=0,$$

$$\frac{\partial}{\partial x}\left(\frac{8}{15}q+\varphi\right)=-\frac{1}{\mathrm{Kn}}\frac{(1-\sigma)\sigma}{T},$$

$$\frac{\partial}{\partial x}\left(\frac{1}{3}\chi+\psi\right)=-\frac{4}{3\mathrm{Kn}}\frac{(1-\sigma)q}{T}, \tag{26}$$

$$\frac{\partial}{\partial x}\left(\frac{9}{35}\psi\right)=-\frac{3}{2\mathrm{Kn}}\frac{(1-\sigma)\varphi}{T},$$

$$\frac{\partial}{\partial x}(28qT)=-\frac{2}{3\mathrm{Kn}}\frac{[1-\sigma)}{T}[\chi-15T(1-\sigma)],$$

$$\frac{\partial}{\partial x}\left(\frac{112}{15}qT+9T\varphi\right)=-\frac{7}{6\mathrm{Kn}}\frac{(1-\sigma)}{T}(\psi-T\sigma).$$

Here, we have introduced the abbreviations $\varphi=u^{\langle 0\rangle}_{\langle 3\rangle},\chi=u^{\langle 2\rangle}_{\langle 0\rangle},\psi=u^{\langle 1\rangle}_{\langle 2\rangle}$. For now, we are interested only in the first-order deviations from a global equilibrium, where $T_E=1,\sigma_E=0,q_E=0,\varphi_E=0,\chi_E=15,\psi_E=0$. That is, we consider the linearized moment equations; numerical solutions of the nonlinear moment equations will be presented later in this paper. Considering only first-order terms in deviations from this equilibrium state, we find

$$q=\mathrm{const},\quad \frac{\partial\varphi}{\partial x}=-\frac{1}{\mathrm{Kn}}\sigma,\quad \frac{\partial}{\partial x}\left(\frac{1}{3}\chi+\psi\right)=-\frac{4}{3\mathrm{Kn}}q,$$

$$\frac{\partial}{\partial x}\left(\frac{9}{35}\psi\right)=-\frac{3}{2\mathrm{Kn}}\varphi,\quad 0=-\frac{2}{3\mathrm{Kn}}[\chi-15(T-\sigma)],$$

$$9\frac{\partial\varphi}{\partial x}=-\frac{7}{6\mathrm{Kn}}(\psi-\sigma),$$

χ and ψ can easily be computed as

$$\chi=15(T-\sigma),\quad \psi=\frac{61}{7}\sigma$$

and the remaining equations reduce to

$$\frac{\partial\varphi}{\partial x}=-\frac{1}{\mathrm{Kn}}\sigma,\quad \frac{\partial}{\partial x}\left(T+\frac{26}{35}\sigma\right)=-\frac{4}{15}\frac{1}{\mathrm{Kn}}q,$$

$$\frac{366}{245}\frac{\partial\sigma}{\partial x}=-\frac{1}{\mathrm{Kn}}\varphi.$$

Since the heat flux is constant, we can integrate the second equation to

$$T=K-\frac{4}{15}\frac{qx}{\mathrm{Kn}}-\frac{26}{35}\sigma, \tag{27}$$

while the two other equations give for the stress

$$\sigma=A\cosh\sqrt{\frac{245}{366}}\frac{x-0.5}{\mathrm{Kn}}+B\sinh\sqrt{\frac{245}{366}}\frac{x-0.5}{\mathrm{Kn}}. \tag{28}$$

A, B, K, and q are the four constants of integration and four boundary conditions are required for their determination. Thus, the two boundary conditions for the wall temperatures—or the temperature jumps, respectively—are not sufficient for a complete solution of the problem.

However, the boundary conditions are not necessary for a general discussion of the result: The first two terms in Eq. (27) give the solution of the linearized Fourier law, i.e., a straight temperature curve. The third term, $-\frac{26}{35}\sigma$, gives the deviation from the Fourier law, due to the influence of the higher moments. Our numerical results in Sec. V suggest that the leading term in the stress is given by

$$\hat{\sigma}=-B\sinh\sqrt{\frac{245}{366}}\frac{x-0.5}{\mathrm{Kn}}$$

and Fig. 3 shows this function for various Knudsen numbers (arbitrary units, normalized). It can be seen that this deviation has the form of a Knudsen boundary layer indeed. Evidently, the thickness of the boundary layer increases with the Knudsen number.

It must be emphasized that in the case of one-dimensional stationary heat transfer the Burnett equations for Maxwell molecules [21] reduce to the Fourier law (22) and, therefore, cannot describe a linear boundary layer, see Ref. [26] for details.

IV. KINETIC SCHEME

A. The scheme

We present our own derivation of the numerical scheme [9]. While in Refs. [13,14] the authors start from the Boltzmann equation, our argument is based on the moment equa-

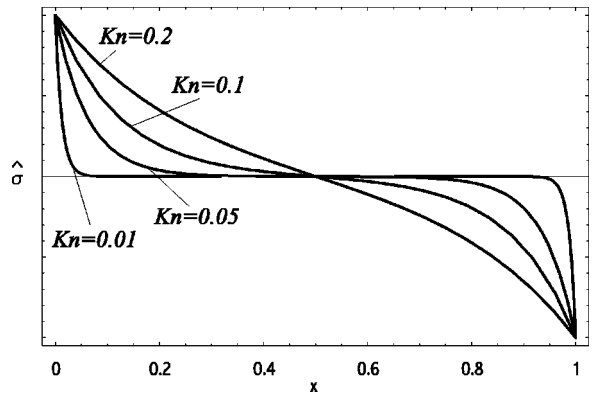

FIG. 3. Function $\hat{\sigma}$ for various Knudsen numbers Kn (arbitrary units) computed from the eight-moment case.

tions plus the definitions of moments, fluxes and productions, and the knowledge of the moment solution for the phase density.

For the discretization in space we consider an interval $x \in (0,L)$ divided in n parts of length $\Delta x = L/n$, with center points x^i, $i=1,\ldots,n$. We write the one-dimensional moment Eq. (12) as

$$\frac{\partial u_A}{\partial t} + \frac{\partial F_A}{\partial x} = P_A$$

and integrate along Δx to obtain

$$\frac{\partial u_A^i}{\partial t} + \frac{1}{\Delta x}\int_{x^i-\Delta x/2}^{x^i+\Delta x/2} \frac{\partial F_A}{\partial x} dx = P_A^i \tag{29}$$

with the cell averages

$$u_A^i = \frac{1}{\Delta x}\int_{x^i-\Delta x/2}^{x^i+\Delta x/2} u_A\, dx \quad \text{and} \quad P_A^i = \frac{1}{\Delta x}\int_{x^i-\Delta x/2}^{x^i+\Delta x/2} P_A\, dx.$$

The interval around x^i is associated with one value u_A^i and the moment solution for the phase density in Δx is determined by this value, $f^i = f(u_A^i, c_k)$. We consider the integral in Eq. (29), which yields

$$\int_{x^i-\Delta x/2}^{x^i+\Delta x/2} \frac{\partial F_A}{\partial x} dx = F_A^{i+1/2} - F_A^{i-1/2},$$

where $F_A^{i\pm 1/2} = F_A(x^i \pm \Delta x/2)$ denote the fluxes at the borders of the interval. We consider the definition (6b) and decompose the flux into its parts due to particles traveling in positive or negative x direction, respectively,

$$\begin{aligned} F_A^{i+1/2} &= \int \psi_A c_x f^{i+1/2}\, d\boldsymbol{c} \\ &= \int_{c_x \geqslant 0} \psi_A c_x f^{i+1/2}\, d\boldsymbol{c} + \int_{c_x \leqslant 0} \psi_A c_x f^{i+1/2}\, d\boldsymbol{c}. \end{aligned} \tag{30}$$

Here, the first integral describes the flux of ψ_A from x^i towards x^{i+1} and the second integral gives the flux from x^{i+1} into x^i.

The key step of the method is the assumption that the flux out of x^i is determined by the state in cell i, while the flux into the cell i is determined by the state in the neighboring cell, $i+1$. This assumption may be written as

$$\int_{c_x \geqslant 0} \psi_A c_x f^{i+1/2}\, d\boldsymbol{c} \simeq A_A^i, \quad \int_{c_x \leqslant 0} \psi_A c_x f^{i+1/2}\, d\boldsymbol{c} \simeq B_A^{i+1}, \tag{31}$$

where the half-fluxes in positive and negative directions A_A^i and B_A^i are defined as

$$A_A^i = \int_{c_x \geqslant 0} \psi_A c_x f^i d\boldsymbol{c}, \quad B_A^i = \int_{c_x \leqslant 0} \psi_A c_x f^i\, d\boldsymbol{c}. \tag{32}$$

Now, Eq. (30) reads

$$F_A^{i+1/2} = A_A^i + B_A^{i+1}$$

and we obtain the space discretized moment equations as

$$\frac{\partial u_A^i}{\partial t} + \frac{1}{\Delta x}(A_A^i + B_A^{i+1} - A_A^{i-1} - B_A^i) = P_A^i, \quad i=1,\ldots,n. \tag{33}$$

Following Le Tallec and Perlat, we consider discrete times $t^j = j\Delta t$ with time step Δt and use a time-splitting method, i.e., we solve transport and relaxation consecutively. We denote $u_A^i(t^j) = u_A^{i,j}$. Then, the time splitting is as follows:

(a) Transport step. With $u_A^{i,j}$ as initial condition solve

$$\frac{\partial u_A^i}{\partial t} + \frac{1}{\Delta x}(A_A^i + B_A^{i+1} - A_A^{i-1} - B_A^i) = 0$$

during Δt, with result $\tilde{u}_A^{i,j+1}$.

(b) Relaxation step. With $\tilde{u}_A^{i,j+1}$ as initial condition solve

$$\frac{\partial u_A^i}{\partial t} = P_A^i$$

during Δt, with result $u_A^{i,j+1}$. Repeat both steps to go on in time.

The solution of the scheme for the variables u_A^i, $i=1,\ldots,n$ requires:

(i) Constitutive equations for the half-fluxes and the productions

$$A_A^i = A_A^i(u_B^i), \quad B_A^i = B_A^i(u_B^i), \quad P_A^i = P_A^i(u_B^i);$$

these follow from the definitions (32) and (11) and the moment solution (13).

(ii) Initial values for the moments $u_A^{i,0}$.

(iii) Boundary conditions, i.e., the half-fluxes A_A^0 and B_A^{n+1}, which follow from the boundary conditions for the phase density. According to the boundary condition (3), these are the half-fluxes of the wall-distribution function $\theta f_W + (1-\theta) f_N(-n_k c_k)$, where f_W is the wall Maxwellian, and f_N denotes the moment solution in front of the wall. One obtains

$$A_A^0 = \theta A_A^{0,W} - (1-\theta)\phi_A B_A^1,$$

$$B_A^{n+1} = \theta B_A^{n+1,W} - (1-\theta)\phi_A A_A^n,$$

where $A_A^{0,W}, B_A^{n+1,W}$ are the half fluxes of the two wall Maxwellians and $\phi_A = \psi_A(-c_x)/\psi_A(c_x)$ (the entries in ϕ_A are either $+1$ or -1).

The constitutive equations for the half-fluxes $A_A(u_B)$, $B_A(u_B)$ as well as the boundary conditions A_A^0, B_A^{n+1} are computed from the phase density with a MATHEMATICA® program, and directly saved as a FORTRAN subroutine. We shall not give any details on these functions, see Ref. [9] for details of the 13- and 14-moment cases.

Most of our numerical calculations are based on a first-order scheme, with a simple Euler time step, viz.,

$$u_A^{i,j+1} = u_A^{i,j} + \Delta t P_A^{i,j} - \frac{\Delta t}{\Delta x}(A_A^{i,j} + B_A^{i+1,j} - A_A^{i-1,j} - B_A^{i,j}). \tag{34}$$

The implementation of the semi-implicit scheme for the relaxation step used in Refs. [9,13] is too cumbersome for the large numbers of moments in questions, and was not used. However, its implementation is easy for the BGK production terms (14), and then it is the best choice.

The evolution of temperature follows from the balance of internal energy (20), and its discretized form differs from Eq. (34), viz.,

$$T^{i,j+1} = T^{i,j} \exp\left[-\frac{2}{3}\frac{\Delta t}{\Delta x}\frac{1}{1-\sigma^{i,j}} \times (A_\varepsilon^{i,j} + B_\varepsilon^{i+1,j} - A_\varepsilon^{i-1,j} - B_\varepsilon^{i,j}) \right].$$

In principle, it poses no problem to consider this finite volume scheme—where only half-space moments of the fluxes are used—for multidimensional processes. This feature distinguishes the Grad method with kinetic schemes from other methods where half-space moments are taken as variables, e.g., the Mott-Smith method [40], or a similar method that was used in Ref. [41] for the simulation of the heat transfer problem. Moreover, these methods are not very systematic, since it is not clear *a priori* which moment equations one should use in order to obtain the equations for the half-space variables.

B. Accuracy and limitations

In order to show that the above discretization is of first order in space we expand

$$u_A^i = u_A, \quad A_A^i = A_A,$$

$$A_A^{i\pm1} = A_A \pm \frac{\partial A_A}{\partial x}\Delta x + \frac{\partial^2 A_A}{\partial x^2}\frac{(\Delta x)^2}{2}, \text{ etc.},$$

and obtain with $A_A + B_A = F_A$ from Eq. (33)

$$\frac{\partial u_A}{\partial t} + \frac{\partial F_A}{\partial x} - \frac{\Delta x}{2}\frac{\partial^2 (A_A - B_A)}{\partial x^2} = P_A + O((\Delta x)^2).$$

In Ref. [9] we showed that Δx must be small compared to the mean free path of the gas, so that the method can only be used for relatively large Knudsen numbers. This fact is partly related to the kinetic schemes, but also reflects the stiffness of the moment equations. However, extended sets of moment equations are required in the particular case of large Knudsen numbers, so that the restriction is not severe. Moreover, the resolution of Knudsen boundary layers requires a grid size below the mean free path anyway.

In the first-order scheme, moments and phase density are approximated as piecewise constant functions in space. A second-order scheme can be obtained by constructing piecewise linear functions with the minmod reconstruction [42]. We set

$$\text{minmod}(u_A^i) = \frac{1}{2}[\text{sgn}(u_A^{i+1} - u_A^i) + \text{sgn}(u_A^i - u_A^{i-1})] \times \min[(u_A^{i+1} - u_A^i), (u_A^i - u_A^{i-1})]$$

and

$$u_A(x) = u_A^i + \text{minmod}(u_A^i)\frac{x - x_i}{\Delta x},$$

$$x_i - \frac{\Delta x}{2} < x < x_i + \frac{\Delta x}{2}.$$

The scheme (33) requires the half-fluxes $A_A(u_B), B_A(u_B)$ at the cell boundaries, see Eq. (31). These are now obtained as

$$A_A^i = A_A[u_B^i + \tfrac{1}{2}\text{minmod}(u_B^i)],$$

$$B_A^i = B_A[u_B^i - \tfrac{1}{2}\text{minmod}(u_B^i)].$$

For consistency, we used the modified Euler method (method of Heun) for second-order integration in time.

In the following section we shall present results with Knudsen numbers Kn$=0.01,0.05,0.1,0.2,0.5,1$. The second-order scheme was used for Kn$=0.01$ with 200 grid points, and for Kn$=0.05$ with 100 grid points. All other results rely on the first-order scheme with 100 grid points. The CFL number $\Delta t/\Delta x$ was chosen between 0.05 and 0.1. The initial values for the moments correspond to a global equilibrium with the temperature of the left wall being $T_0 = 1$. The temperature of the right wall is increased linearly until the final temperature T_L is reached. Then, the calculation is continued until the stationary state is reached. The necessary number of time steps n varies with the Knudsen number, for Kn$=0.5$ we had $n = 16\,000$ (heating period $n/4$) while $n = 160\,000$ was needed for Kn$=0.01$ (heating period $n/2$).

C. Accuracy at the wall

In the case of one-dimensional stationary heat transfer the heat flux should be constant in space. However, independent

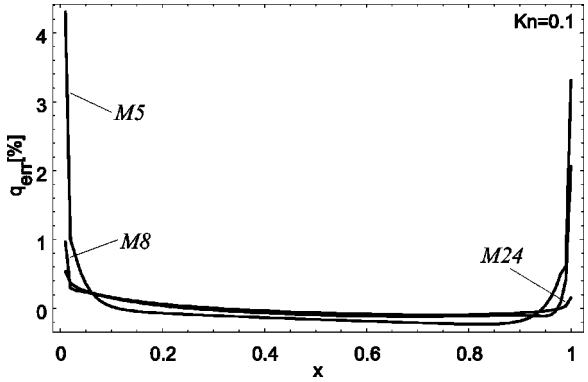

FIG. 4. Deviation of heat flux from its mean value (in %) for theories with 5, 8, and 24 moments, Kn$=0.1$, $T_0=1$, $T_L=1.5$.

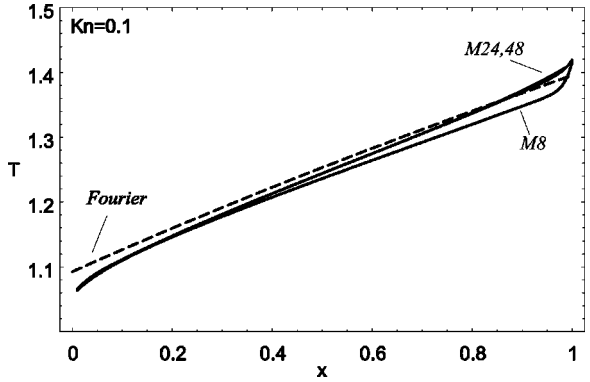

FIG. 5. Temperature curve for moment theories with 8, 24, 48 moments and Fourier solution (dashed), Kn$=0.1$, $T_0=1$, $T_L=1.5$, and $\theta=1$.

of the accuracy of the scheme, we observe jumps in the heat flux at the wall, which stand in contradiction to the conservation of energy. The jumps in the heat flux are a consequence of the moment approximation and the kinetic schemes, and cannot be avoided. In order to see this, we study Eq. (33) for the left cell ($i=1$) in the stationary state,

$$A_A^1+B_A^2-A_A^0-B_A^1=\Delta x P_A^i. \tag{35}$$

If the fields were continuous between cells 1 and 2, we had $B_A^1=B_A$, $B_A^2\simeq B_A+dB_A/dx\,\Delta x$ and for $\Delta x\to 0$ Eq. (35) would reduce to the requirement $A_A^1=A_A^0$. This gives as many equations as there are variables (moments), and accordingly the values of all moments at the wall were prescribed. In particular, the heat flux would assume different values at the two walls. This is extremely unphysical: the heat flux must adjust itself to a constant value that depends on the temperature difference between the walls. This dilemma is avoided by jumps of the fields between the two cells next to the wall.

Our results show that the jumps in the heat flux become smaller with increasing number of moments. Figure 4 shows the deviation of the heat flux from its mean value for various number of moments for the parameters Kn$=0.1, T_0=1, T_L=1.5$ (for full accommodation, $\theta=1$). With only five moments, the jump is about 4%, but it is less than 0.5% with 24 moments. With the present choice of parameters, a further increase of the moment number leads to only small improvements. The profiles close to the wall follow from the finite step size Δx. With a finer grid, the curves reduce to a constant line with two jumps at the walls, see Ref. [9] for corresponding results.

In order to understand the improvement due to the increase of the number of moments better, one has to recall that the moment method assumes a moment solution (7) in all space points, i.e., a series. According to the boundary condition (3), the phase density at the wall is a discontinuous function of the microscopic velocity. A series in polynomials, which pictures this discontinuity sufficiently, will require a large number of expansion coefficients, i.e., moments.

V. RESULTS AND DISCUSSION

A. Influence of the moment number

We start the survey of our results with some figures that show the influence of the number of moments. Again, we consider the case with Kn$=0.1$, $T_0=1$, $T_L=1.5T$, and $\theta=1$. Figure 5 shows the temperature curves computed with 8, 24, and 48 moments in comparison to the Fourier solution (23). There is no marked difference between the 24- and 48-moments cases, but the eight-moment case differs significantly. This difference becomes even more apparent, when we consider other moments, e.g., the anisotropic stress σ, see Fig. 6, or the nonequilibrium part of the fourth moment $\Delta=\int c^4(f-f_M)d\boldsymbol{c}$, see Fig. 7.

For the discussion of the stress σ one should bear in mind, that $\sigma=0$ in the Navier-Stokes case. Nonzero values of σ therefore are related to Knudsen number effects, in our case to the Knudsen boundary layer. Again, we find almost the same results for moment numbers above 24 moments. The corresponding boundary layer structure is stretched far into the gas and is independent of the grid size. Notice, however, that σ contributes less than 1% to the total stress $p_0=1$.

With eight and five moments we find smaller structures close to the wall, which depend on the grid size, and will reduce to jumps, if the grid is more and more refined. These structures are a consequence of the jumps in the heat flux at

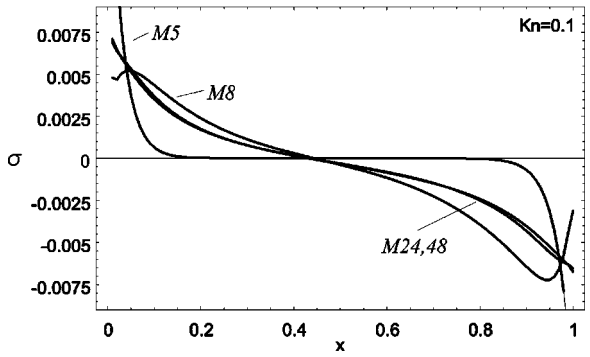

FIG. 6. Anisotropic stress σ for various numbers of moments, Kn$=0.1$, $T_0=1$, $T_L=1.5$, and $\theta=1$.

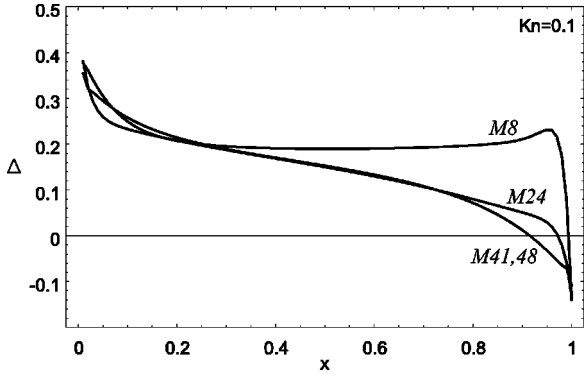

FIG. 7. Nonequilibrium part Δ of fourth moment for various numbers of moments, Kn$=0.1$, $T_0=1$, $T_L=1.5$, and $\theta=1$.

the walls, i.e., improper boundary conditions, and have no physical meaning. Recall that σ should vanish in the five-moment case.

The nonequilibrium part Δ of the fourth moment is another quantity that will be zero in local equilibrium, i.e., in the range of validity of the Navier-Stokes theory. Figure 7 shows that Δ is considerably different from zero, and that it is more sensitive to a change of the number of moments, the curves obtained with 24 and 48 moments now are slightly different. The results converge with increasing number of moments: there is no visible discrepancy between the results obtained with 41 and 48 moments, respectively.

Under the assumption of constant pressure, as in Refs. [10–12], it follows that in dimensionless form

$$\Delta=\frac{56}{5}q^2\simeq 0.192=\text{const},$$

where the numerical value holds for the present example. As can be seen, this value is realized in the bulk for the eight-moment case, while for higher moment numbers Δ is a strictly descending function. Clearly, in our solution, Δ is dominated by boundary effects that were excluded in Refs. [10–12].

We already discussed the jumps of the heat flux in Sec. IV C. Figure 8 shows the mean value of q as it changes with the number of moments α as defined in Eq. (8). One can see the convergence of the heat flux towards a constant value for

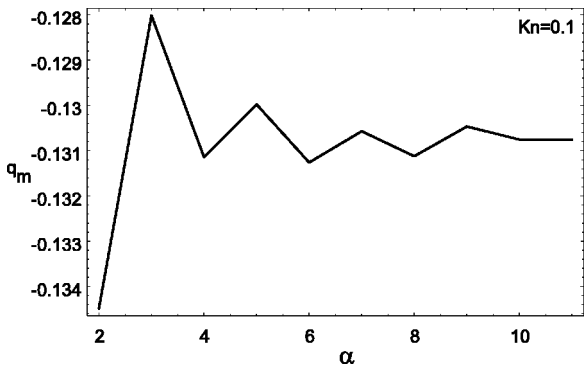

FIG. 8. Mean value of heat flux over number of moments α Eq. (8), Kn$=0.1$, $T_0=1$, $T_L=1.5$, and $\theta=1$.

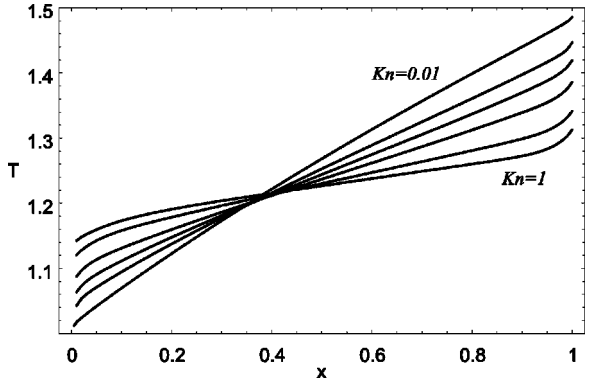

FIG. 9. Temperature curve for Knudsen numbers Kn $=0.01,0.05,0.1,0.2,0.5,1$, wall temperatures $T_0=1$, $T_L=1.5$, and $\theta=1$.

increasing number of moments. The zig-zag shape of the curve indicates some differences between sets with even and odd values of α.

B. Influence of Knudsen number

Now we turn our attention to the influence of the Knudsen number. Figure 9 shows the temperature for a variety of Knudsen numbers between Kn$=0.01$ and Kn$=1$, again for the wall temperatures $T_0=1$,$T_L=1.5$. All curves were calculated with sufficiently large moment numbers, so that the results did not change when more moments were added. The figure must be compared with Fig. 2, which shows the results for the Fourier case. Evidently, the moment solution gives smaller jumps, and adds marked boundary layers.

In order to emphasize the difference between Fourier and moment solution, we show a direct comparison for Kn $=0.01$ and Kn$=1$ in Fig. 10. For the smaller Knudsen number, Kn$=0.01$, there is no visible difference between the two results. The boundary layer effects can be ignored and also the jumps are negligible. We conclude that for Knudsen numbers Kn$\leqslant 0.01$ the gas can be described by the Fourier theory with sufficient accuracy. For higher Knudsen numbers, however, one has to account for the rarefaction of the gas by more and more moments, since only then one can

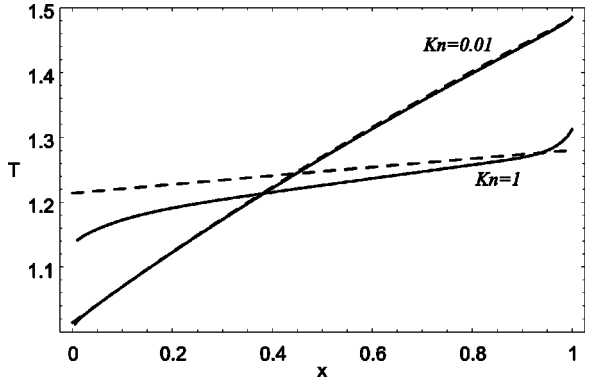

FIG. 10. Comparison of moment solution with Fourier solution, Kn$=0.01$ and Kn$=1$.

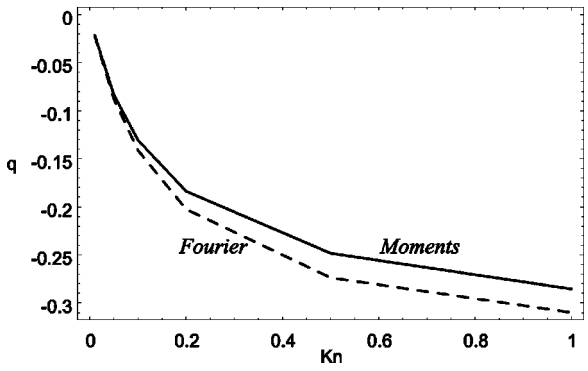

FIG. 11. Heat flux q over Knudsen number Kn for wall temperatures $T_0=1$, $T_L=1.5$. Continuous line, moment solution; discontinuous line, Fourier solution (25).

expect a proper description of the temperature jumps and boundary layers.

Figure 11 shows the heat flux as a function of the Knudsen number, again comparing Fourier case and many moments. The Fourier law overestimates the heat flux by about 10% compared to the moment approach.

The growth of the boundary layer with increasing Kn can best be seen from the curves of the anisotropic stresses in Fig. 12. With $\mathrm{Kn}=0.01$ the stress indeed differs from zero only in a small layer at the walls. With increasing Kn the boundary layer expands more and more into the gas. Already at $\mathrm{Kn}=0.1$ both boundary layers meet, and the rarefied gas effects dominate the anisotropic stresses σ.

For Knudsen numbers $\mathrm{Kn}\geqslant 1$, collisions among the gas particles are less frequent than interactions between particles and the walls, so that the transfer of heat is dominated by the free flight of the gas particles between the walls. In this case, the convergence of the moment equations with increasing moment number is rather weak. According to our simulations, a number of 48 moments seems not to be sufficient in the case $\mathrm{Kn}=1$.

Additionally, some of the moment systems become unstable for large Knudsen numbers, which leads to large oscillations in the heat flux or complete breakdown of the code. However, this happens only for the moment systems (8) with α even and $\alpha\geqslant 6$. Remember that already Fig. 8 indicated that systems with α even or odd have different properties. At present it is not clear whether the instabilities are a property

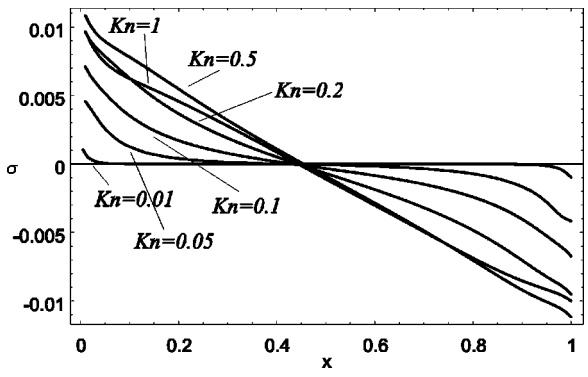

FIG. 12. Anisotropic stresses for various Kn.

of the equations, or of the equations *and* the use of the kinetic schemes.

C. Comparison with the work by Ohwada

So far we have shown the general behavior of our extended moment systems. In this section we address the question whether our solutions correspond to solutions of the Boltzmann equations. Although there are many papers available, which address stationary heat transfer in rarefied gases, we could not find a reference where exactly the same problem is solved, i.e., stationary heat transfer in a gas of Maxwellian molecules with Maxwell boundary conditions [44]. Indeed, authors who use DSMC simulations or solve the Boltzmann equation by other means prefer to consider hard sphere interaction between molecules, while authors working with moment equations prefer Maxwellian molecules, as we do in the present work. With solutions for Maxwellian molecules lacking, we decided to compare our results with those of Ohwada [18] for hard sphere molecules, obtained by a discretization method, developed by Sone and co-workers [3]. In our dimensionless units, Ohwada considers stationary heat transfer for wall temperatures $T_0=0.86, T_L=1.14$ with accommodation coefficient $\theta=0.826$ and/or $\theta=0.5$ for Knudsen numbers $\mathrm{Kn}^{HS}=0.0658,0.1395,0.1942,0.2994,0.7582$. For hard sphere molecules, Knudsen number and heat conductivity are related by [2]

$$\mathrm{Kn}^{HS}=\frac{32}{75}\sqrt{\frac{2}{\pi}}\frac{\kappa}{p_0 L}\sqrt{\frac{m}{k}T_0},$$

while for Maxwellian molecules we obtain from Eqs. (15) and (19)

$$\mathrm{Kn}=\frac{4}{15}\frac{\kappa}{p_0 L}\sqrt{\frac{m}{k}T_0}.$$

We wish to compare gases with the same heat conductivity, and thus we find for the relation between the Knudsen numbers,

$$\mathrm{Kn}=\frac{5}{8}\sqrt{\frac{\pi}{2}}\mathrm{Kn}^{HS}, \tag{36}$$

that is, in order to have results comparable with those of Ohwada, we have to consider the Knudsen numbers $\mathrm{Kn}=0.051\,54,0.1093,0.1521,0.2345,0.5939$. Figure 13 shows the temperature curves from the moment theory (48 one-dimensional moments) in juxtaposition to those of Ohwada. The black dots on the right and left are an identical set, and have been introduced to guide the eye. Obviously, for the small Knudsen numbers ($\mathrm{Kn}=0.051\,54, \mathrm{Kn}^{HS}=0.0658$), both methods give identical results. As the Knudsen numbers are increased, we observe small differences between the two sets of solutions, which are more marked directly at the wall. These small differences might be due to an insufficient moment number, to the fact that we considered the linearized collision term of the Boltzmann equation, or to the differences in the interaction potential.

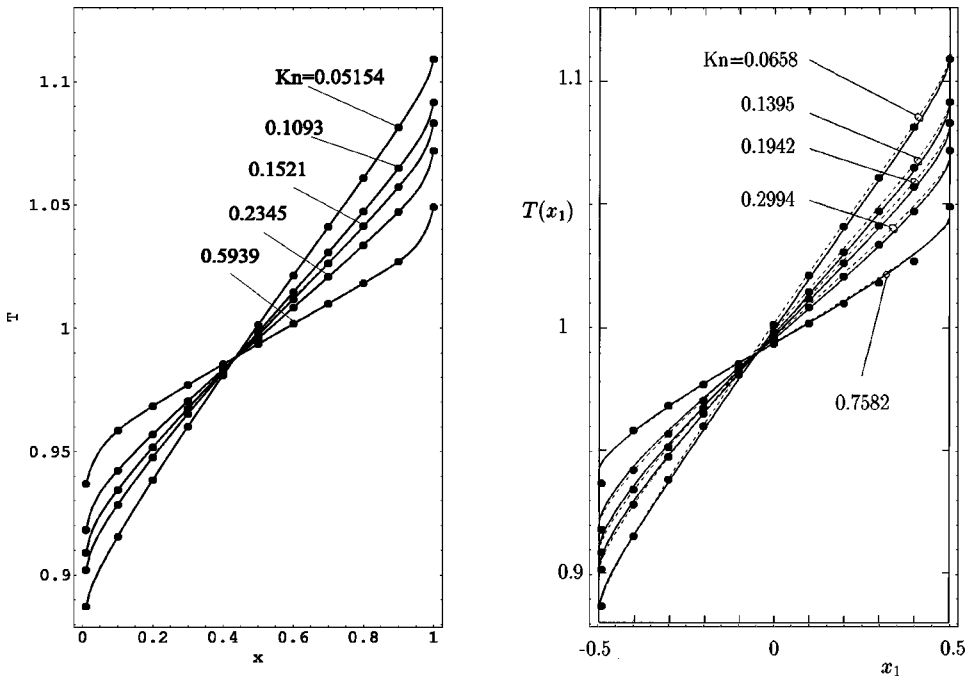

FIG. 13. Temperature distribution for stationary heat transfer between two plates with accommodation coefficient $\theta=0.826$. Left: Moment solutions for Maxwellian molecules. Right: Solutions of the Boltzmann equation for hard sphere molecules (continuous lines) and BGK equation (broken line) by Ohwada [18]. The Knudsen numbers correspond to the same heat conductivity, see Eq. (36). The black dots on the right correspond to those on the left.

Figure 14 shows the density distribution for the same Knudsen numbers with accommodation coefficients $\theta_0=0.826$ at the right wall, and $\theta_L=0.5$ at the right wall. In order to compare our results with those of Ohwada, we plot the rescaled density $\hat{\varrho}(\hat{x})/\hat{\varrho}(0.5)$. Again, we can observe a good agreement between moment solutions and solutions of the Boltzmann equation with small differences in the vicinity of the walls and for larger Knudsen numbers.

D. Influence of temperature difference

So far, we presented results for a moderate temperature ratio between the two walls, $T_L/T_0=1.5$. Now we ask what happens, when the temperature ratio is increased. Figure 15 shows the temperature curve for $T_L/T_0=2.5$ at Kn$=0.1$ for several moment numbers up to 48. Our simulations indicate that the results have not yet converged, and more moments would be needed in order to describe the process properly. Note the marked difference between the moment solutions and the solution of the Fourier law (dashed).

A further increase of the temperature ratio leads to a breakdown of the code, and thus the method cannot be used in these cases. The breakdown is probably due to an insufficient resolution of the discontinuous phase density at the walls. It should be emphasized, however, that for applica-

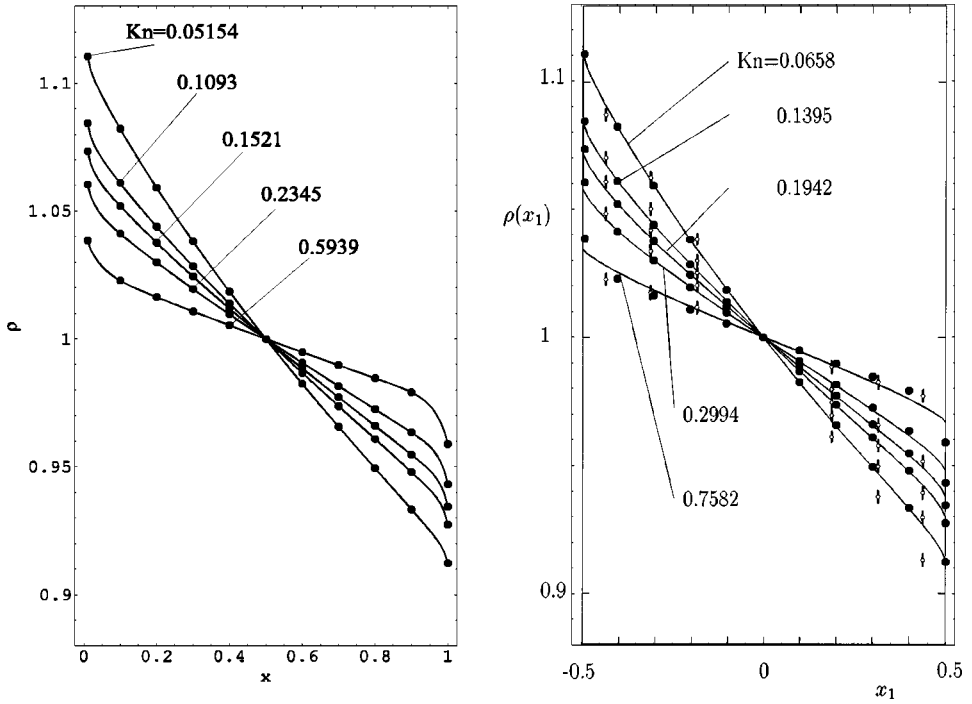

FIG. 14. Density distribution for stationary heat transfer between two plates with accommodation coefficients $\theta_0=0.826$, $\theta_L=0.5$. Left: Moment solutions for Maxwellian molecules. Right: Solutions of the Boltzmann equation for hard sphere molecules (continuous lines) and BGK equation (broken line) by Ohwada [18]. The Knudsen numbers correspond to the same heat conductivity, see Eq. (36). The black dots on the right correspond to those on the left.

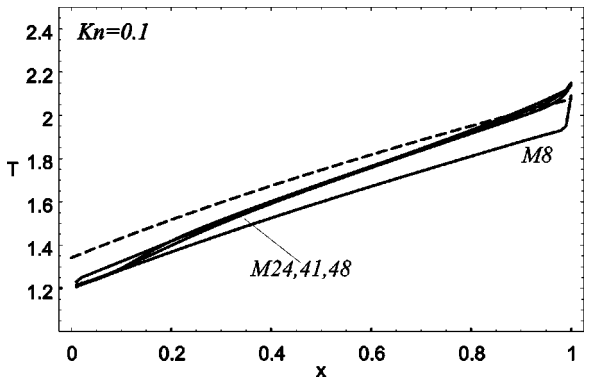

FIG. 15. Temperature curve for moment theories with 8, 24, 41, 48 moments and Fourier solution (dashed), Kn$=0.1$, $T_0=1$, $T_L=2.5$, and $\theta=1$.

tions in MEMS and microchannels the temperature ratio will be close to 1.

Due to the restriction to relatively small temperature differences we cannot compare our results with those in Refs. [5,29,30,41] where the authors consider temperature ratios above 10. From these papers it seems that the linear boundary layers are less important at large temperature differences while the overall behavior is mostly driven by the nonlinear terms in the heat flux equation.

VI. CONCLUSIONS

In the present paper, we considered moment equations that are based on the Boltzmann equation with the linearized collision operator for Maxwellian molecules and closed by the method of Grad. We have solved the stationary heat transfer problem for the moment equations numerically with the method of kinetic schemes. This method allows to implement the boundary condition for the Boltzmann equation, so that the boundary conditions for the moments are well defined for any set of moment equations.

Our results show that the method gives satisfying results—including temperature jumps and Knudsen boundary layers in fair agreement with direct solutions of the Boltzmann equation—in the transition regime (Knudsen numbers $0.01 \leqslant \mathrm{Kn} \leqslant 1$) at moderate temperature differences between the walls. These are the conditions one will meet in the simulation of MEMS and microchannels, so that Grad's method may be a suitable tool here. The reentry problem of spacecrafts, however, involves strong gradients, and requires the resolution of shocks. There, the description with moment equations requires a huge amount of equations, and the method is more of theoretical than practical interest, e.g., see [37] for the calculation of shock profiles.

However, our results show that one has to consider a relatively large number of moments to obtain satisfactory results. This will prevent the use of the method for more complicated problems, e.g., problems involving complex geometries. The large number is needed mostly in order to ensure the conservation laws at the walls. It is likely, although not guaranteed, that one can find alternative methods to implement the boundary conditions, which might allow accurate simulations of jumps and boundary layers with a smaller number of moments. Only with these one will consider the moment equations as a tool for technical applications. Modified boundary conditions will be discussed elsewhere.

Flow problems with nonzero velocity are more important in the simulation of MEMS and microchannels. Thus, the next step in line is to apply the Grad method with kinetic schemes to standard flow problems, e.g., Couette and Poiseuille flow. For these, one will observe velocity slip at the walls and boundary layers in the velocity in addition to the temperature jumps and boundary layers of this paper; see Ref. [20] for an account of boundary layers in the Couette flow for the 26-moment case and Ref. [32] for a discussion of slip in moment systems. The analysis of these flow problems will follow the same lines as outlined here for the heat transfer problem.

In any case, our results show that Grad's moment systems—other than the Burnett equations—contain the important features of boundary dominated processes in the transition regime, and we hope that they will play an important role in the future simulation of microscopic flow phenomena.

ACKNOWLEDGMENTS

I wish to thank Dr. Jörg Au (Technical University of Berlin) for the code that was used in the calculation of the production terms. This study was carried out during a long-term stay at the Institute for Mathematics and its Applications (IMA) during its program on ''Reactive Flow and Transport Phenomena,'' and I wish to thank the IMA for their hospitality and support. This research was supported by the Natural Sciences and Engineering Research Council of Canada (NSERC).

[1] C. Cercignani, *Theory and Application of the Boltzmann Equation* (Scottish Academic Press, Edinburgh, 1975).

[2] S. Chapman and T.G. Cowling, *The Mathematical Theory of Non-Uniform Gases* (Cambridge University Press, Cambridge, 1970).

[3] Y. Sone, T. Ohwada, and K. Aoki, Phys. Fluids A **1**, 363 (1989).

[4] G. Bird, *Molecular Gas Dynamics and the Direct Simulation of Gas Flows* (Clarendon Press, Oxford, 1994).

[5] D.W. Mackowski, D.H. Papadopoulos, and D.E. Rosner, Phys. Fluids **11**, 2108 (1999).

[6] H. Grad, Commun. Pure Appl. Math. **2**, 325 (1949).

[7] I. Müller and T. Ruggeri, *Rational Extended Thermodynamics*, Springer Tracts in Natural Philosophy Vol. 37 (Springer, New York, 1998).

[8] H. Struchtrup, Ann. Phys. (San Diego) **257**, 111 (1997).

[9] H. Struchtrup, ZAMP **51**, 346 (2000).

[10] E.S. Asmolov, N.K. Makashev, and V.I. Nosik, Dokl. Akad. Nauk. SSR **249**, 577 (1979) [Sov. Phys. Dokl. **24**, 892 (1979)].

[11] A. Santos, J.J. Brey, C.S. Kim, and J.W. Dufty, Phys. Rev. A

39, 320 (1989).
[12] M. Tij, V. Garzo, and A. Santos, Phys. Rev. E **56**, 6729 (1997).
[13] P. Le Tallec and J. P. Perlat (unpublished).
[14] B. Perthame, SIAM (Soc. Ind. Appl. Math.) J. Numer. Anal. **27**, 1405 (1990).
[15] M. Junk, *Kinetic Schemes—A New Approach and Applications* (Shaker-Verlag, Aachen, 1997).
[16] W. Dreyer, J. Phys. A **20**, 6505 (1987).
[17] C.D. Levermore, J. Stat. Phys. **83**, 1021 (1996).
[18] T. Ohwada, Phys. Fluids **8**, 2153 (1996).
[19] D. Risso and P. Cordero, Phys. Rev. E **56**, 489 (1997); **57**, 7365(E) (1998).
[20] D. Reitebuch and W. Weiss, Continuum Mech. Thermodyn. **11**, 227 (1999).
[21] J.H. Ferziger and H.G. Kaper, *Mathematical Theory of Transport Processes in Gases* (North-Holland, Amsterdam, 1972).
[22] A.V. Bobylev, Dokl. Akad. Nauk. SSR **262**, 71 (1982) [Sov. Phys. Dokl. **27**, 29 (1982)].
[23] P. Rosenau, Phys. Rev. A **40**, 7193 (1989).
[24] K.A. Comeaux, D.R. Chapman, and R.W. MacCormack, AIAA Report No. 95-0415, 1995 (unpublished).
[25] H. Struchtrup, J. Thermophys. Heat Transfer **15**, 372 (2001).
[26] H. Struchtrup (unpublished).
[27] M. N. Kogan, *Rarefied Gas Dynamics* (Plenum Press, New York, 1969).
[28] Y. Sone, C. Bardos, F. Golse, and H. Sugimoto, Eur. J. Mech. B/Fluids **19**, 325 (2000).
[29] J.M. Montanero, M. Alaoui, A. Santos, and V. Garzó, Phys. Rev. E **49**, 367 (1994).
[30] C.S. Kim, J.W. Dufty, A. Santos, and J.J. Brey, Phys. Rev. A **39**, 328 (1989).
[31] H. Struchtrup and W. Weiss, Phys. Rev. Lett. **80**, 5048 (1998).
[32] H. Struchtrup and W. Weiss, Continuum Mech. Thermodyn. **12**, 1 (2000).
[33] E. Barbera, I. Müller, and M. Sugiyama, Meccanica **34**, 103 (1999).
[34] J. Au, I. Müller, and T. Ruggeri, Continuum Mech. Thermodyn. **12**, 19 (2000).
[35] W. Dreyer, M. Junk, and M. Kunik (unpublished).
[36] L. Waldmann, *Transporterscheinungen in Gasen von Mittlerem Druck*, edited by S. Flügge, Handbuch der Physik XII: Thermodynamik der Gase (Springer, Berlin, 1958).
[37] J.D. Au, Ph.D. thesis, TU Berlin, 2001.
[38] C. Truesdell and R.G. Muncaster, *Fundamentals of Maxwell's Kinetic Theory of a Simple Monatomic Gas* (Academic Press, New York, 1980).
[39] R. L. Liboff, *The Theory of Kinetic Equations* (Wiley, New York, 1969).
[40] H.M. Mott-Smith, Phys. Rev. **82**, 885 (1951).
[41] P.-J. Clause and M. Mareschal, Phys. Rev. A **38**, 4241 (1988).
[42] E. F. Todo, *Riemann Solvers and Numerical Methods for Fluid Mechanics* (Springer, Berlin, 1997).
[43] A constitutive equation for the mass flux is not needed since the mass flux equals the momentum density, and thus is contained in $u_A^{[5]}$ already.
[44] The author would be more than pleased to hear about numerical solutions of this problem. Please mail bibliographical data to struchtr@me.uvic.ca